Physics Procedia

Volume 75, 2015, Pages 1181–1186

20th International Conference on Magnetism

Magnetic Properties and Crystal Structure of $DyMn_2O_5$ Nanoparticles Embedded in Mesoporous Silica

T. Tajiri[1*], Y. Ando[2], H. Deguchi[2], M. Mito[2], and A. Kohno[1]

[1] *Faculty of Science, Fukuoka University, Fukuoka, Japan*

[2] *Faculty of Engineering, Kyushu Institute of Technology, Kitakyushu, Japan*

tajiri@fukuoka-u.ac.jp

Abstract

We synthesized $DyMn_2O_5$ nanoparticles with the nanometer size using mesoporous silica as template of nanoparticles. The size effects of the $DyMn_2O_5$ nanoparticles were investigated through crystal structure analysis and magnetic measurement. The powder X-ray diffraction measurement revealed that the synthesized nanoparticles have orthorhombic structure with particle size of approximately 7 nm. The lattice constants for the nanoparticles deviated from those for the bulk crystal. The $DyMn_2O_5$ nanoparticles exhibited superparamagnetic behaviors. The evaluated Weiss temperature for the nanoparticles was positive value, whereas that for bulk crystal was negative one. The experimental results suggested that the distortion of crystallographic structure in the nanoparticles induced the changes in magnetic exchange interactions and magnetic frustration among manganese spins.

Keywords: $DyMn_2O_5$, nanoparticles, crystal structure, superparamagnetic, magnetic interaction

1 Introduction

Magnetic nanoparticles show interesting magnetic behavior owing to the changes in their energy state and crystal structure at the surface of the nanoparticles, contributed to the finite size effect and surface effect. In particular, strong correlated materials are expected to exhibit unique size effects, because these compounds have strong correlation among charge, spin, orbital, and lattice degrees of freedom. In our previous studies, we synthesized the RMnO$_3$ (R = (La, Sr), Dy, Bi) nanoparticles with particle size of about 8–15 nm and investigated their crystal structure and magnetic properties. [1, 2, 3, 4] These nanoparticles exhibited the unique size effects such as changes in magnetic transition temperature, magnetic phase, magnetic interactions and crystallographic structure from those for bulk crystal. It is considered that these unique size effects were attributed to the strong correlation between magnetic properties and crystal structure.

* Corresponding author

Selection and peer-review under responsibility of the Scientific Programme Committee of ICM 2015

doi:10.1016/j.phpro.2015.12.117

In the present study, we focused on the size effects of magnetic properties and crystal structure on $DyMn_2O_5$. $DyMn_2O_5$ is strong correlated oxide and has been known as a multiferroic material. The crystallographic symmetry of $DyMn_2O_5$ is orthorhombic symmetry with space group *Pbam*. The $DyMn_2O_5$ has linked $Mn^{4+}O_6$ octahedra and $Mn^{3+}O_5$ pyramids. The $Mn^{4+}O_6$ octahedra share edges to form ribbons parallel to the *c* axis, adjacent ribbons being linked by pairs of corner-shearing $Mn^{3+}O_5$ pyramids. [5, 6, 7] $DyMn_2O_5$ shows a complex magnetoelectric phase diagram with such as commensurate-incommensurate transition. [6, 8, 9, 10, 11, 12] The Mn moment shows antiferromagnetic order below T_N(Mn) ≈ 42 K. The incommensurate-commensurate transition at T_N' ≈ 30 K is caused by competing exchange interactions. Dy spins ordered below T_N(Dy) ≈ 8 K. To the best our knowledge, there have been no reports of magnetic properties and crystal structure of $DyMn_2O_5$ nanoparticles based on detailed systematic experimental studies. In this paper, we report the successful synthesis of the $DyMn_2O_5$ nanoparticles with particle size of about 7 nm and their magnetic properties and crystal structure. We demonstrated the size effects on physical properties, associated with superparamagnetism, magnetic blocking phenomena, and distortion of crystallographic structure from that for bulk crystal.

2 Experiment

The $DyMn_2O_5$ nanoparticles were synthesized in one-dimensional pores with diameter of about 7 nm of mesoporous silica SBA-15 which was using as a template to equalize the particle size during the fabrication of the $DyMn_2O_5$ nanoparticles. SBA-15 has a well-ordered two-dimensional hexagonal mesoporous structure, and the one-dimensional pores are separated by silica walls. [13] The $DyMn_2O_5$ nanoparticles were synthesized by soaking the SBA-15 in a stoichiometric aqueous solution of $Dy(CH_3COO)_3$•$4H_2O$ and $Mn(CH_3COO)_2$•$4H_2O$. Then, the soaked samples were dried and calcinated in oxygen atmosphere.

Powder X-ray diffraction (XRD) measurements for the $DyMn_2O_5$ nanoparticles in SBA-15 were carried out at room temperature using the synchrotron radiation X-ray diffractometer with a Debye-Scherrer camera at the beamline BL-8B of Photon Factory (PF), Institute of Materials Structure Science, High Energy Accelerator Research Organization (KEK), Japan. The incident X-ray wavelength was 0.68814 Å calibrated using CeO_2 powder XRD pattern. The magnetic properties of the $DyMn_2O_5$ nanoparticles in SBA-15 were investigated using a superconducting quantum interference device (SQUID) magnetometer (Quantum Design MPMS).

3 Experimental results and discussion

We observed powder XRD patterns for $DyMn_2O_5$ nanoparticles synthesized in the pores of SBA-15. Figure 1 shows the powder XRD pattern of the $DyMn_2O_5$ nanoparticles in SBA-15 subtracting backgrounds, glass capillary and SBA-15, and simulated patterns for $DyMn_2O_5$ and Dy_2O_3 bulk crystal at room temperature. The obtained XRD pattern exhibited some broad Bragg peaks, which were corresponding to those for $DyMn_2O_5$ bulk crystal with orthorhombic symmetry. [5, 6, 7] The powder XRD patterns included some Bragg peaks attributable to the impurity compound Dy_2O_3 indicated by asterisk symbols in Figure 1. The average crystallite size for the $DyMn_2O_5$ nanoparticles was estimated based on the peak positions and the full width at half maximum of the seven Bragg peaks for $2\theta \leq 30^\circ$ using Scherrer's equation. The estimated size was the same as the pore size of SBA-15. These results indicated successful synthesis of the $DyMn_2O_5$ nanoparticles with average particle size of 7.2 ± 0.7 nm in the pores of SBA-15.

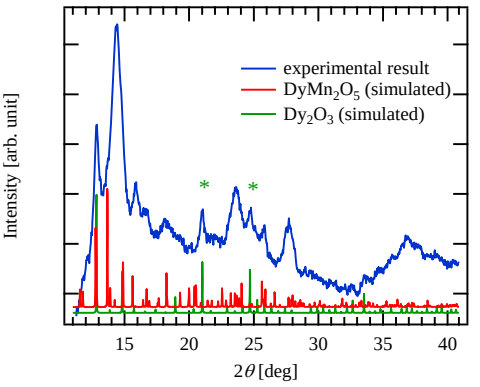

Figure 1: Powder XRD pattern for the $DyMn_2O_5$ nanoparticles in SBA-15 and simulated patterns for $DyMn_2O_5$ and Dy_2O_3 bulk crystal at room temperature. Asterisk symbol indicates the impurity phase of Dy_2O_3.

The lattice constants for the $DyMn_2O_5$ nanoparticles were estimated from the powder XRD patterns. The lattice constant *a* obtained via the peak angles of Bragg peaks was 7.23(1) Å that is smaller than those for bulk crystal, whereas the lattice constant *b* was 8.64(1) Å that is larger than that for bulk crystal. The lattice constant *c* was 5.68(1) Å, that is almost the same value with that for bulk crystal. These results indicated that the crystallographic structure for the nanoparticles distorted from that for bulk crystal. [7]

Figure 2 shows the temperature dependence of the dc magnetic susceptibilities for the $DyMn_2O_5$ nanoparticles in the pores of SBA-15. The dc magnetic susceptibilities were measured under an external magnetic field H = 100 Oe in both field-cooling (FC) and zero-field-cooling (ZFC) conditions. Both the FC and ZFC susceptibilities increased as temperature decreased. Below 10 K, the rapid increase of both the FC and ZFC susceptibilities was attributed to the magnetic ordering among the Dy

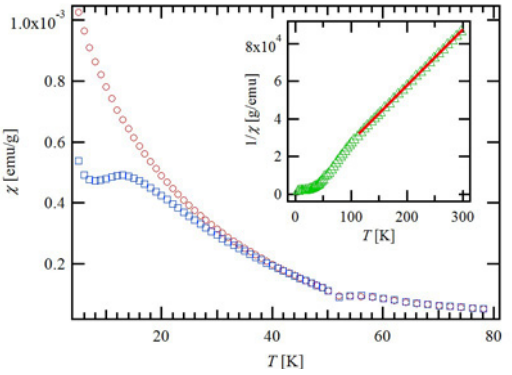

Figure 2: Temperature dependence of dc magnetic susceptibilities for $DyMn_2O_5$ nanoparticles in SBA-15 under an external magnetic field of H = 100 Oe in field-cooled (circle symbols) and zero-field-cooled condition (square symbol). Inset shows temperature dependence of inverse susceptibility. The solid line represents the Curie-Weiss law with Weiss temperature of approximately 7 K.

spins in $DyMn_2O_5$ nanoparticles. The anomaly around 55 K was due to the magnetic anomaly of accidentally adsorbed oxygen in pores of SBA-15. The temperature dependence of magnetic susceptibilities exhibited a pronounced magnetic irreversibility between FC and ZFC susceptibilities below 35 K. The FC susceptibility increased continuously with decreasing temperature, whereas ZFC susceptibility exhibited a hump around 15 K. It is considered that these behaviors attributed to blocking phenomena of superparamagnetism derived from the magnetic ordering of Mn moments in the $DyMn_2O_5$ nanoparticles, because nonlinear magnetic susceptibility calculated from ac susceptibility did not exhibit a critical divergence at the temperature where hysteresis started between the FC and the ZFC susceptibilities. In our study, the magnetic transition temperatures for the nanoparticles could not be determined through the magnetic measurement for randomly oriented nanoparticles, because it is impossible to obtain the magnetic transition temperatures only from the magnetic measurement results. It was expected that, for the $DyMn_2O_5$ with the intricate interplay of multiple magnetic Mn-Mn spin interactions, the magnetic interactions for the nanoparticles change from that for bulk crystal as observed for the $BiMnO_3$ nanoparticles. [4] For high temperature region, $T > 100$ K, the Mn moments dominate the magnetic susceptibility for the $DyMn_2O_5$ nanoparticles. The fit to the Curie-Weiss law to the temperature dependence of inverse susceptibility up to 300 K is shown by solid line in inset of Figure 2. The Weiss temperature estimated from fitting to the Curie-Weiss law was approximately 7 K, which had opposite sign from that for bulk crystal. This result suggested that the magnetic exchange interaction network due to the Mn moments for the nanoparticles changed from those for bulk crystal.

Figure 3 shows magnetization curves for $DyMn_2O_5$ nanoparticles in SBA-15 at 5 and 15 K. At temperatures of below the blocking temperature T_B = 35 K, the $DyMn_2O_5$ nanoparticles exhibited a hysteresis loop owing to blocking phenomena of the superparamagnetic particles. The magnitude of magnetization and coercive field H_c increased, H_c = 278 and 68 Oe at 5 and 15 K, respectively, with decreasing temperature. The magnetization curves for the nanoparticles at 5 and 15 K were well reproduced by the Langevin function of the solid lines in Figure 3. These behaviors implied that the $DyMn_2O_5$ nanoparticles exhibited superparamagnetic behavior. These results were consistent with the temperature dependence of susceptibility.

The magnetic measurement results indicated that the $DyMn_2O_5$ nanoparticles with particle size of approximately 7 nm in the pores of SBA-15 have different Weiss temperature from that for bulk crystal. The lattice constants for the nanoparticles deviated slightly from that for bulk crystal, which indicated that the crystallographic structure for the nanoparticles distorted anisotropically from that for

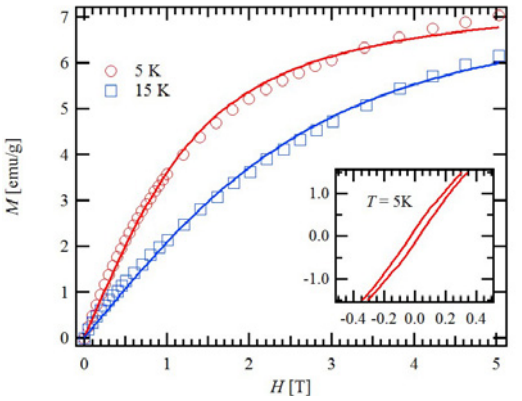

Figure 3: Magnetization curves for the $DyMn_2O_5$ nanoparticles in SBA-15 at 5 and 15 K. Solid lines indicate the Langevin function curves fitted to the measurement results. Inset shows magnification of the low field region of the hysteresis loop with H_c = 278 Oe at 5 K.

bulk crystal. It is likely that the unique magnetic size effect results from the change in crystallographic structure. The $DyMn_2O_5$ have the complex magnetic phase diagram owing to the intricate interplay of at least five magnetic Mn-Mn spin interactions in the geometrically frustrated structure. [6, 9, 14] It is considered that the distortion of crystallographic structure of the nanoparticles induced the changes in magnetic exchange interaction network and magnetic frustration between Mn spins. For RMn_2O_5 (R=Tb, Ho, Dy) bulk crystal, such structural distortion and modulation in magnetic phase depend strongly on the radius of R. [6] The size effect of the $DyMn_2O_5$ nanoparticles has the results similar to that in R displacement for bulk RMn_2O_5. In order to elucidate the magneto-structural correlation in the $DyMn_2O_5$ nanoparticles, we are planning to conduct the theoretical calculation by the first principle calculation.

4 Conclusion

We synthesized the $DyMn_2O_5$ nanoparticles with particle size of approximately 7 nm in mesoporous silica SBA-15 to investigate their magnetic properties and crystal structure. The powder XRD measurement results indicated successful fabrication of $DyMn_2O_5$ nanoparticle with mean particle size of approximately 7 nm. The crystallographic structure for the nanoparticles was distorted from that for bulk crystal. The magnetic measurement results for the $DyMn_2O_5$ nanoparticle in SBA-15 exhibited the superparamagnetic behavior. The estimated Weiss temperature for the nanoparticles was positive value and had opposite sign from that for bulk crystal. The distortion of crystallographic structure in the nanoparticles induced changes in magnetic exchange interaction network and magnetic frustration among Mn spins, which resulted in the appearance of different magnetic state.

Acknowledgements

This work was supported by a Grant-in-Aid for Young Scientists (B) (No. 25870999) and Grant-in-Aid for Scientific Research (C) (No. 26390010) from the Ministry of Education, Culture, Sports, Science and Technology (MEXT) of Japan. The synchrotron radiation experiments were performed at the BL-8B beamline located at the Photon Factory (Proposal No. 2011G511 and 2013G523).

References

[1] T. Tajiri, H. Deguchi, S. Kohiki, M. Mito, S. Takagi, K. Tsuda, Y. Murakami, Journal of Physical Society of Japan 75, 113704, 2006.

[2] T. Tajiri, H. Deguchi, S. Kohiki, M. Mito, S. Takagi, M. Mitome, Y. Murakami, A. Kohno, Journal of Physical Society of Japan 77, 074715, 2008.

[3] T. Tajiri, N. Terashita, K. Hamamoto, H. Deguchi, M. Mito, Y. Morimoto, K. Konishi, A. Kohno, Journal of Magnetism and Magnetic Materials 345, 288, 2013.

[4] T. Tajiri, M. Harazono, H. Deguchi, M. Mito, A. Kohno, S. Kohiki, Japanese Journal of Applied Physics 49, 06GH04, 2010.

[5] C. Wilkinson, F. Sinclair, P. Gardner, J. B. Forsyth, B. M. R. Wanklyn, J. Phys. C: Solid State Phys. 14, 1671, 1981.

[6] G. R. Blake, L. C. Chapon, P. G. Radaelli, S. Park, N. Hur, S-W. Cheong, J. Rodríguez-Carvajal,

Phys. Rev. B 71, 214402, 2005.

[7] S. C. Abrahams, J. L. Bernstein, J. Chem. Phys. 46, 3776, 1967.

[8] W. Ratcliff II, V. Kiryukhin, M. Kenzelmann, S.-H. Lee, R. Erwin, J. Schefer, N. Hur, S. Park, S-W. Cheong, Phys. Rev. B 72, 060407(R), 2005.

[9] N. Hur, S. Park, P. A. Sharma, S. Guha, S-W. Cheong, Phys. Rev. Lett. 93, 107207, 2004.

[10] R. A. Ewings, A. T. Boothroyd, D. F. McMorrow, D. Mannix, H. C. Walker, B. M. R. Wanklyn, Phys. Rev. B 77, 104415, 2008.

[11] Z. Y. Zhao, M. F. Liu, X. Li, J. X. Wang, Z. B. Yan, K. F. Wang, and J.-M. Liu, J. Appl. Phys. 116, 054104, 2014.

[12] C. R. dela Cruz, F. Yen, B. Lorenz, M. M. Gospodinov, C. W. Chu, W. Ratcliff, J. W. Lynn, S. Park, S.-W. Cheong, Phys. Rev. B 73, 100406(R), 2006.

[13] D. Zhao, J. Feng, Q. Huo, N. Melosh, G. H. Fredrickson, B. F. Chemlka, G. D. Stucky, Science 279 548, 1998.

[14] T. Shen, K. Cao, G.-C. Guo, L. He, Phys. Rev. B 78, 134413, 2008.